J. Membrane Biol. 79, 119–134 (1984)

The Journal of
Membrane Biology

A Study of Dynamic Membrane Phenomena During the Gastric Secretory Cycle: Fusion, Retrieval and Recycling of Membranes

Carlos Jirón, Mirtha Romano and Fabián Michelangeli
Centro de Biofísica y Bioquímica, Instituto Venezolano de Investigaciones Científicas (IVIC), Caracas 1010A, Venezuela

Summary. The possibility of recycling, fusion and retrieval of membranes during the gastric secretory process was studied in isolated gastric mucosae of the toad *Bufo marinus*. Incorporation and efflux of ^{14}C-inulin and horseradish peroxidase (HRP) into the tissue as well as transmission and freeze-fracture electron microscopic studies during the secretory cycle were done. HRP and ^{14}C-inulin were incorporated into the tubulovesicular membrane system during the secreting-resting transition. Upon restimulation, markers were released towards the lumen. Marker efflux preceded onset of H^+ secretion. Morphological transformations in the oxyntic cell as evidenced from transmission and freeze-fracture electron microscopy preceded acid secretion coinciding with marker efflux. At this time, images that have been associated with membrane fusion were found in the apical membranes of oxyntic cells. The results are consistent with a model where membrane area increases by a fusion mechanism at the expense of the tubulovesicular system. This transformation precedes the onset of H^+ secretion. Upon cessation of the stimulus or inhibition, membranes are retrieved and the tubulovesicular system reformed. Retrieved membranes could be then reutilized in the next secretory cycle.

Key Words membrane fusion · membrane recycling · oxyntic cell · gastric mucosa · H^+ transport · *Bufo marinus*

Introduction

Stimulation of the acid secretory process in the gastric oxyntic cell leads to morphological transformations that have been evidenced in a number of vertebrate species [10]. This ubiquitous phenomenon is characterized by a large increase in apical cell membrane area with a concomitant reduction in the intracellular tubulovesicular (TV) system of membranes [18]. The increase in apical cell membrane area appears to occur at the expense of the intracellular TV system [15, 16]. This transformation is reversible upon withdrawal of the stimulus or inhibition of acid secretion [32, 35, 40].

The mechanism by which the area of the apical membrane increases at the expense of the TV system is not known. Fusion of the TV system with the apical membrane has been postulated by several authors [4, 14].

The regeneration of the TV system may result from two alternative mechanisms, either new synthesis of membranes or reversal of the process involving retrieval of the exposed membranes during the secreting-resting transition. Some results that can be interpreted as endocytosis of exposed membranes in the gastric mucosa can be found in the literature [34]. If this is the case then it would seem likely that the retrieved membranes may be reutilized in the next secretory cycle. Recycling of membranes has been postulated as a mechanism for membrane conservation in a variety of secretory tissues, both of neural and nonneural origin [8, 9, 19, 20, 21, 29, 31]. Furthermore, membrane recycling has been shown to occur in cells engaged in pinocytotic activity. An extensive review on this subject has recently appeared [38]. Important evidence for such a mechanism has been obtained in those tissues studied by incorporation of electron-dense markers into endocytic vesicles and following its intracellular fate by electron microscopy. Forte et al. [14] postulated a membrane recycling hypothesis in this tissue based on electron microscopic examination of the oxyntic cell at various times during the secretory cycle.

Taking into account the extensive membrane transformations that occur during the secretory cycle, the gastric mucosa may serve as a useful model in which to study membrane retrieval and recycling phenomena. Theoretically, one should be able to incorporate fluid phase markers into the endocytosed membrane vesicle and subsequently, after washout of the extracellular space, follow the efflux of the marker and the secretory parameter upon a new stimulation. In an ideal system then, the extent of catabolism and recycling of membranes could be evaluated by this method.

In this study, by using radioactive and electron-dense markers we provide evidence for retrieval and reutilization of membranes during the gastric secretory cycle. The results show that markers are incorporated into the membrane elements of the TV system of the oxyntic cells and subsequently discharged into the gland lumen upon restimulation. The onset of morphological transformations, as evidenced from marker efflux and transmission and freeze-etching electron microscopy, precedes the onset of acid secretion. This phenomenon appears to occur as a result of membrane fusion.

Materials and Methods

General Methods

Gastric mucosae of the toad (*Bufo marinus*) were used for the experiments. Animals were captured in the northern part of Venezuela and maintained in tanks under running tap water until use. After pithing, the stomachs were removed and opened along the lesser curvature. The mucosal layer separated from the muscle coat was split into two halves and mounted as a flat sheet between two Lucite® Ussing-type chambers and bathed with physiological solutions at room temperature. The exposed area was 2 cm^2 and the volume of each chamber 3 ml. The serosal or nutrient solution contained (in mM): 85 NaCl, 4 KCl, 0.8 $MgSO_4$, 1.8 $CaCl_2$, 11 glucose and 25 Tris buffer, pH 7.2. The solution added to the mucosal or secretory side was 120 mM NaCl unless otherwise stated. Both solutions were bubbled with 100% O_2 continuously throughout the experiment. Acid secretory rate was measured either by continuous titration of the secretory solution in the chamber by the pH-stat method [7] or by withdrawing the mucosal chamber contents and titrating to pH 7 at given time periods.

Incorporation and Efflux of Radioactive Extracellular Space Tracers

Mucosae were mounted in chambers as described above. The secretory side was exposed to a solution containing ^{14}C-inulin (2 μCi/ml), for a total time of 270 min. During this time the mucosa was first stimulated to secrete acid by the addition of histamine (10^{-4} M) to the serosal side for a period of 120 min in order to induce increase in membrane area [16, 32]. Then, the reversal of the process was obtained by washing out histamine and addition of metiamide (10^{-3} M). This inhibition period lasted for 150 min. To facilitate the reaching of the tracer to the bottom of the gastric glands, the normal water flow (*see* Discussion), was abolished during most of the tracer uptake period [25, 28]. Thus, an osmotic gradient was applied during the final hour of stimulation and the first 2 hr of metiamide inhibition (60 to 240 min). This was done by the addition of sucrose to the serosal solution to a final concentration of 200 mM. Then, the hyperosmotic solution on the nutrient side was replaced by normal nutrient solution for another 30 min (240 to 270 min) to allow osmotic recovery. There was a very small transepithelial flux of ^{14}C-inulin during the period. Thus, to avoid accumulation of the tracer on the serosal side, the nutrient solution was renewed every 30 min.

At the end of the 270-min incorporation period, 100-μl samples were taken from both bathing solutions to assess specific activity of ^{14}C. Then, the chambers were thoroughly washed by renewal of bathing solutions every minute during 10 min (270 to 280 min). Subsequently, the mucosal solution was replaced every 10 min with fresh solutions. Aliquots were used for liquid scintillation counting of ^{14}C and rate of acid secretion by titration with 0.01 N NaOH in an autotitrator (Radiometer). In initial experiments it was determined that 100 min was more than sufficient for washout of the extracellular space and to obtain a very small amount of radioactivity efflux. Thus, the effect of secretagogues on ^{14}C efflux was studied after 110 min of washout of radioactivity.

Transmission Electron Microscopy

Ultrastructural studies were carried out at different times during the secretory cycle. Mucosae were mounted in chambers as described above. Resting tissue was obtained by prolonged incubation [23], or by incubating in the presence of metiamide [2, 36]. After reaching the resting state by either method, one hemimucosa was stimulated by the addition of secretagogues, while the other was kept as a control. Tissues in the resting state and at various times after stimulation were rapidly withdrawn from the chambers and immersed in ice-cold 2% glutaraldehyde in 0.1 M cacodylate buffer, pH 7.2. The mucosae were minced to pieces about 1 mm^2 in the glutaraldehyde solution. Fixation was carried out for 3 hr in the cold and then washed in cacodylate buffer for another 4 hr with hourly changes. Subsequently, the pieces were postfixed in 2% OsO_4 for 2 hr, dehydrated in a graded series of alcohol and embedded in Epon 812. Thin sections, cut with diamond knives (IVIC), were stained with uranyl acetate, acid lead citrate and viewed in a Hitachi H500 or a JEOL JEM 100B electron microscope.

Freeze-Fracture Electron Microscopy

Pieces from the same tissues studied by transmission electron microscopy were processed for freeze fracture [26]. Tissue was fixed in glutaraldehyde and washed as described above and then immersed in 30% glycerol in 0.1 M cacodylate buffer for 6 hr. Samples were frozen in Freon 22, cooled to −160°C in liquid nitrogen and then fractured in a JEOL freeze-fracture device (JEOL FED-B). Fractures were done at −120°C and etched at −110°C before shadowing with platinum-carbon electrodes. Platinum-carbon replicas were washed in sodium hypochlorite solution, then in distilled water and recovered in copper grids. The replicas were examined in a JEOL JEM 100B electron microscope.

Studies with Electron-Dense Extracellular Markers

Horseradish peroxidase (HRP) was used as extracellular marker, and incorporated into the tissue in the same manner as for ^{14}C-inulin as described above. The mucosal side was exposed to a solution containing HRP (Sigma Type II, 30 mg/ml) for 150 min. During the first 60 min, the mucosae were stimulated with 10^{-4} M histamine. Then the tissues were treated with 10^{-3} M metiamide to inhibit secretion for the remaining 90 min. At the end of this period HRP solution was washed with fresh nutrient. One hemimucosa was immediately fixed in the resting state, whereas the

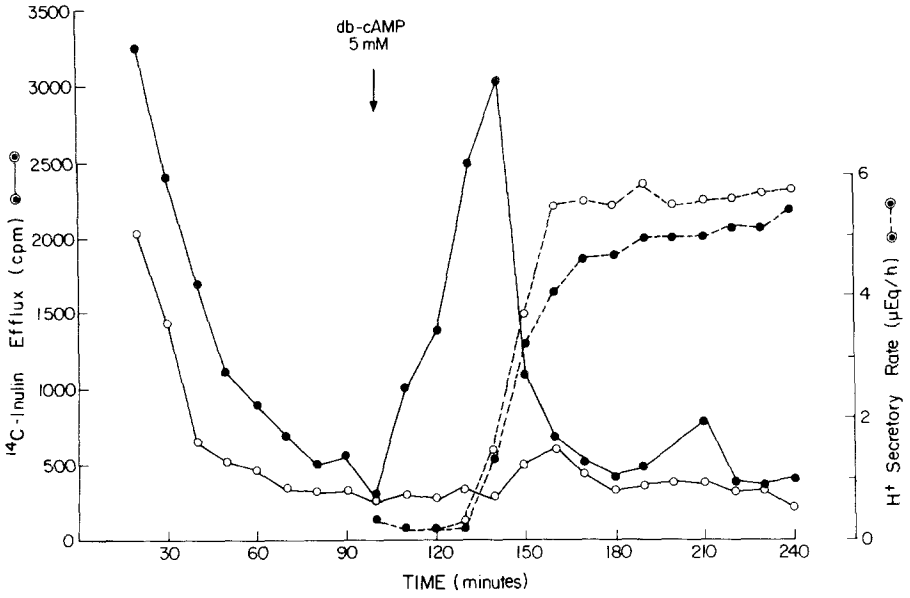

Fig. 1. Effect of db-cAMP (10 mM) on ^{14}C-inulin efflux (continuous lines) and acid secretion (dashed lines) in hemimucosae preloaded with the tracer. One hemimucosae was loaded with the stimulation-inhibition sequence (filled circles) whereas the other was left inhibited with metiamide during the entire loading period (open circles). At the arrow, db-cAMP was added and was present until the end of the experiment. *See* text for details

other one was stimulated again with db-cAMP (10 mM) for 10 min and then fixed. Tissues were minced to small pieces (about 1 mm^2) and fixed in 2% glutaraldehyde in 0.1 M cacodylate buffer pH 7.2, containing 10 mM $CaCl_2$. Fixation was carried out for 3 hr at 1 to 2°C and then the tissues were washed overnight in cacodylate buffer. For histochemical localization of HRP, mucosal pieces were previously cut into 50-μm sections with a vibrotome to assist penetration of the incubation medium. The sections were incubated in a medium containing 0.05% diaminobenzidine, 0.1 M cacodylate buffer, pH 7.2, and 10 mM $CaCl_2$. After 30 min H_2O_2 (0.01%) was added as substrate and incubation carried out for another 45 min at room temperature. After washing for 3 hr in cacodylate buffer, the 50-μm sections were post-fixed in OsO_4, dehydrated in ethanol and embedded in Epon as described above for transmission electron microscopy. Unstained sections were examined in a JEOL JEM 100B electron microscope. Mucosae not exposed to extracellular HRP but incubated in the complete diaminobenzidine medium showed no reaction product except a faint precipitate in mitochondrial cristae (*see* Results).

Results

Radioactive Tracer Efflux Studies

The time course of ^{14}C-inulin efflux, and the effects of stimulation with db-cAMP on tracer efflux and acid secretion, in paired hemimucosae preloaded in two different conditions, are shown in Fig. 1. One hemimucosa was loaded with the tracer with the stimulation-inhibition sequence as described in Materials and Methods, whereas the control one was loaded in the inhibited condition from the beginning. In both hemimucosae, after removal of the tracer, the efflux fell exponentially to very low values with a $t_{1/2}$ of about 7 min, typical of mucosal extracellular space as measured for this tissue [39]. In the experimental half, addition of db-cAMP (10 mM) in the presence of metiamide, induced an increase in tracer efflux which peaked and came down to very low count efflux. There was a temporal dissociation between this phenomenon and acid secretion, the onset of tracer efflux preceding onset of secretion by about 20 to 30 min in most cases. In the control half, little or no count efflux was observed with stimulation despite an elevation of acid secretion to values similar to the experimental half. These effects of restimulation with db-cAMP were common to all secretagogues tested. Joint addition of histamine and theophylline produced an increase in counts and secretion with the temporal dissociation seen with db-cAMP (Fig. 2). If the tubulovesicular system is the compartment where the tracer had accumulated, one might expect a correspondence between the volume estimated from the tracer space and from morphometric calculations. The equivalent volume, released by stimulation represents about one-half of the TV system volume calculated from morphometric measurement (Table 1).

To further study this relationship, the effects of known inhibitors of acid secretion were tested. Paired mucosal halves were used for these experiments. One half was treated with the inhibitor prior to stimulation whereas the other was kept as a control. SCN^- pretreatment completely inhibited the response to db-cAMP in both parameters studied (Fig. 3). An increase in count efflux and secretion with stimulation can be seen in the control half.

Metabolic inhibition by amytal has been shown to depress ATP levels and acid secretion in the iso-

lated amphibian mucosa [30]. Pretreatment with amytal (5 mM) completely abolished the response to db-cAMP both in acid secretion and radioactive tracer efflux (Fig. 4).

Given the anatomical characteristics of the gastric gland, it might be possible that tracer had remained in a space such as the gland lumen. Stimulation of H^+ production with its accompanying volume flow, could sweep out tracer, which could appear preceding H^+ secretion. Experiments were designed to test this possibility. Mucosae, first loaded with ^{14}C-inulin were exposed to a hypertonic solution (S + 200 mM sucrose) on the secretory side after the usual washout of the mucosal extracellular space. Induction of an osmotic water flow by this method did not result in an increased tracer efflux. However, subsequent stimulation with db-cAMP induced radioactivity efflux as in control experiments (*results not shown*).

Table 1 Equivalent volume released upon stimulation in mucosae previously exposed to ^{14}C-inulin

Group[a]	Secretory rate (μeq H^+/hr)[b]	Mucosal wet weight (mg)	Equivalent volume released[c] (μl)	TV system volume[d] (μl)	% of TV system volume released[e]
A	4.4	186.1	3.00	5.57	51
(n = 10)	0.42	18.5	0.6	0.55	
B	3.8	148	0.14	4.43	
(n = 5)	0.48	30.9	0.06	0.92	

[a] Table representing summary of experiments like the one presented in Fig. 1. In group A mucosae were exposed to tracer during a stimulation-inhibition sequence. In Group B, mucosae were exposed to tracer only during inhibition. *See* Materials and Methods for details.

[b] Maximal rate obtained after restimulation with db-cAMP.

[c] Estimated from integration of efflux peak from time 100 to 170 (min after washout) and calculated from specific activity of mucosal bulk solution.

[d] Calculated assuming a TV volume of 2.99% of mucosae. This has been estimated from morphometric measurements (ref. 18; Jirón and Michelangeli, preliminary results).

[e] Calculated from the difference in volume release in the two groups and compared to the TV system volume. Values represent the mean ± SEM.

Transmission Electron Microscopy During the Secretory Cycle

Trying to correlate efflux studies with morphological changes, the structure of the oxyntic cell was studied at different times throughout the secretory cycle. Tissues were fixed in the resting state and at two different times after stimulation with db-cAMP. The first time selected was a few minutes after stimulation when the tissue gave the first sign of H^+ production. This time was coinciding with the peak of ^{14}C-inulin efflux. This is termed presecretory state from here on. Other tissues were fixed after the mucosae had reached a stable secretory rate (≈60 min; secretory state).

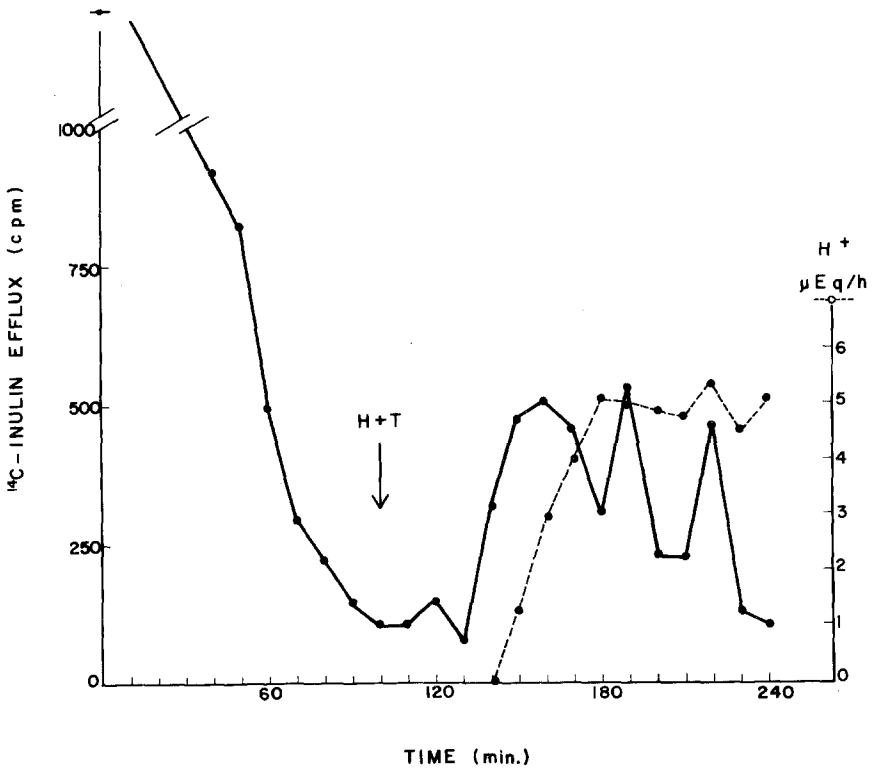

Fig. 2. Effect of histamine (10^{-4} M) plus theophylline (10 mM) on ^{14}C-inulin efflux (continuous lines) and acid secretion (dashed lines) in gastric mucosa preloaded with the tracer. Stimulants were added at the arrow and remained until the end of the experiment

The fine structure of the oxyntic cell of the toad (*Bufo marinus*) in both the resting and secretory states resembles very closely that described for other amphibian species [33]. However, in this work we have found morphological changes at an early stage of stimulation (presecretory state) so far not described in the literature for an amphibian species. Therefore, these changes are briefly described. In this state, structural changes have already started to take place (Fig. 5). It can be observed that numerous microvilli and finger-like processes project from the apical plasma membrane into the gland

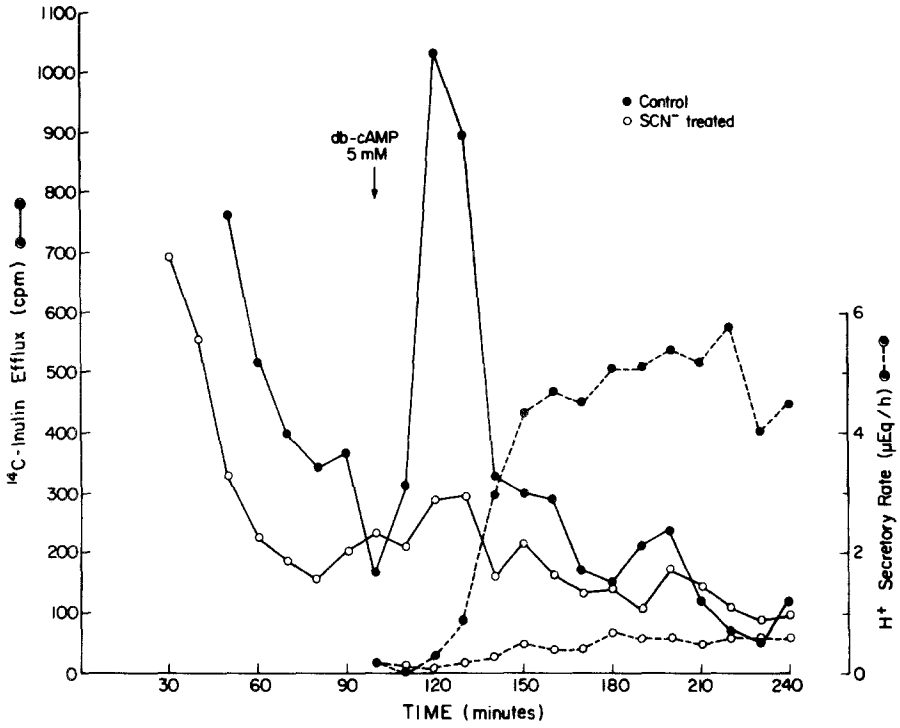

Fig. 3. Effect of SCN^- (20 mM) pretreatment or db-cAMP-induced ^{14}C-inulin efflux (continuous lines) and acid secretion (dashed lines) in gastric hemimucosa preloaded with the tracer. SCN^- was added at zero time and remained until the end of the experiment. The other hemimucosae was kept as a control

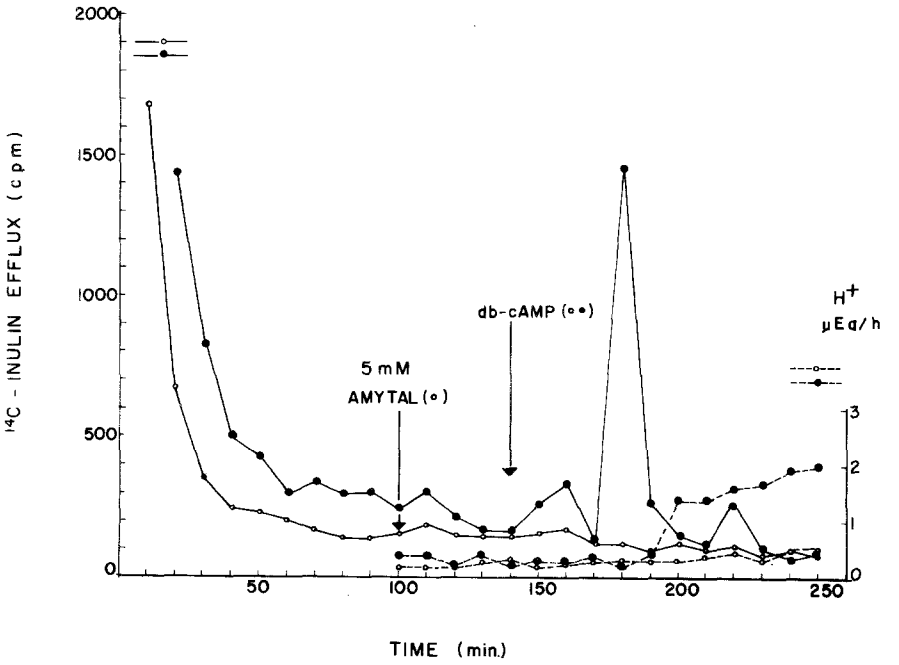

Fig. 4. Effect of amytal (5 mM) pretreatment on db-cAMP-induced ^{14}C-inulin efflux (continuous lines) and acid secretion (dashed lines) in gastric mucosa preloaded with the tracer. Amytal was added to a hemimucosa 40 min prior to the addition of db-cAMP (10 mM). The other hemimucosa was kept as a control

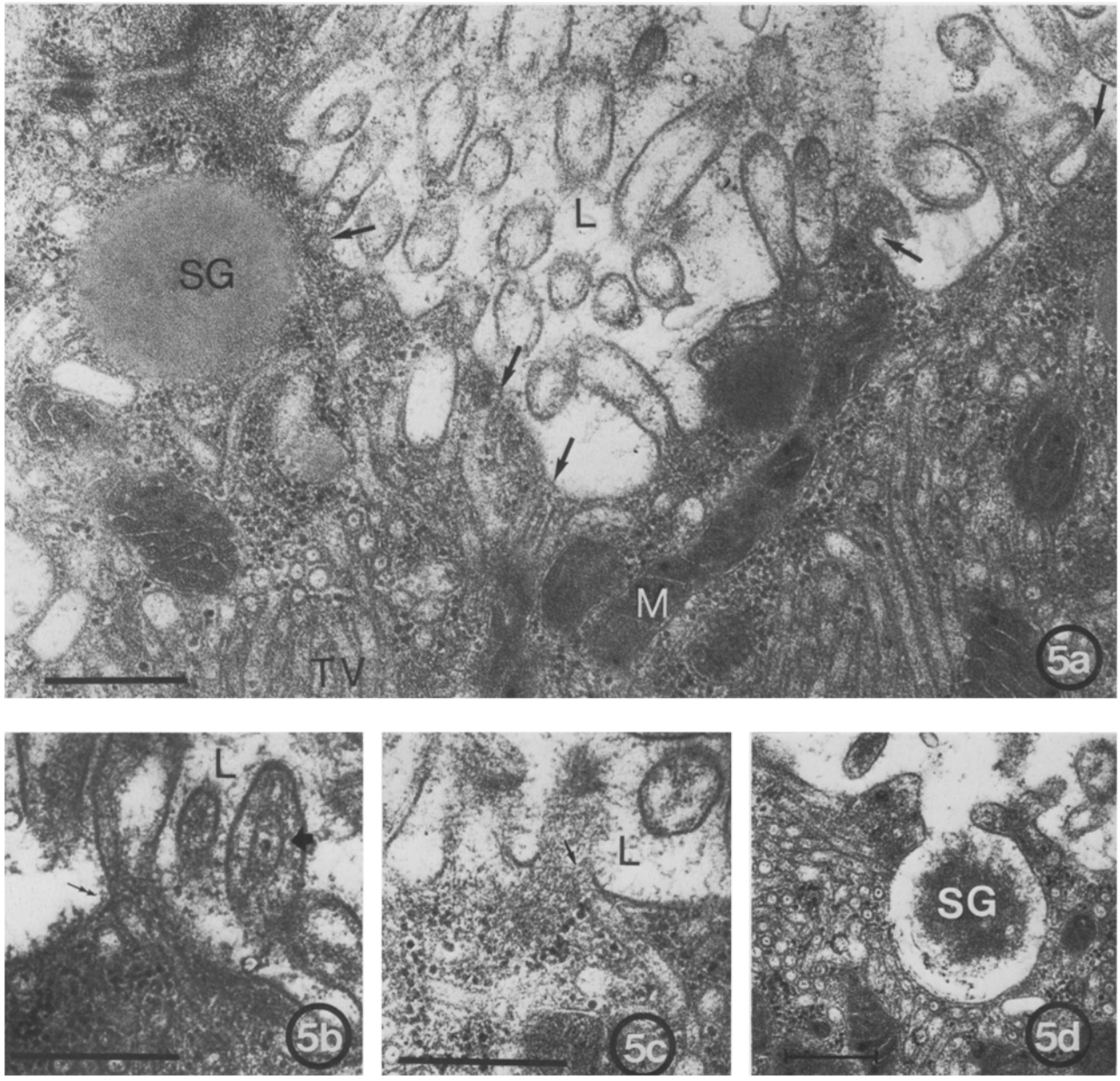

Fig. 5. Apical pole of an oxyntic cell of a toad in the presecretory state. Numerous microvilli project into the gland lumen (*L*). Elements of the TV system (*TV*) are seen in close proximity to the plasma membrane. Images suggestive of fusion are also seen (arrows). Elements of the TV system (*TV*) are seen in contact with the apical plasma membrane or inside microvilli (*5b*). Figure *5c* shows a tubule that is fused with the apical membrane. Exocytosis of secretory granules (*SG*) is seen in this state (*5d*). Bars: 0.5 μm. Magnifications: 42,500× (*5a*), 50,000× (*5b,c*) and 27,000× (*5d*)

lumen greatly increasing the membrane area. Numerous tubular and vesicular elements of the TV system are now seen in close proximity or contacting the apical plasma membrane. In some cases one can see tubular elements inside microvilli or opening into the gland lumen (Fig. *5b–c*). Secretory granules move toward the apex of the cell and exocytosis of these granules (Fig. *5d*) already occurs during this period.

Freeze-Fracture Electron Microscopy During the Secretory Cycle

Freeze-fracture replicas from the same tissues processed for transmission electron microscopy in different physiological states were studied.

The ultrastructure of the toad oxyntic cell as seen in conventional electron microscopy could be easily recognized in freeze-fracture replicas (Figs.

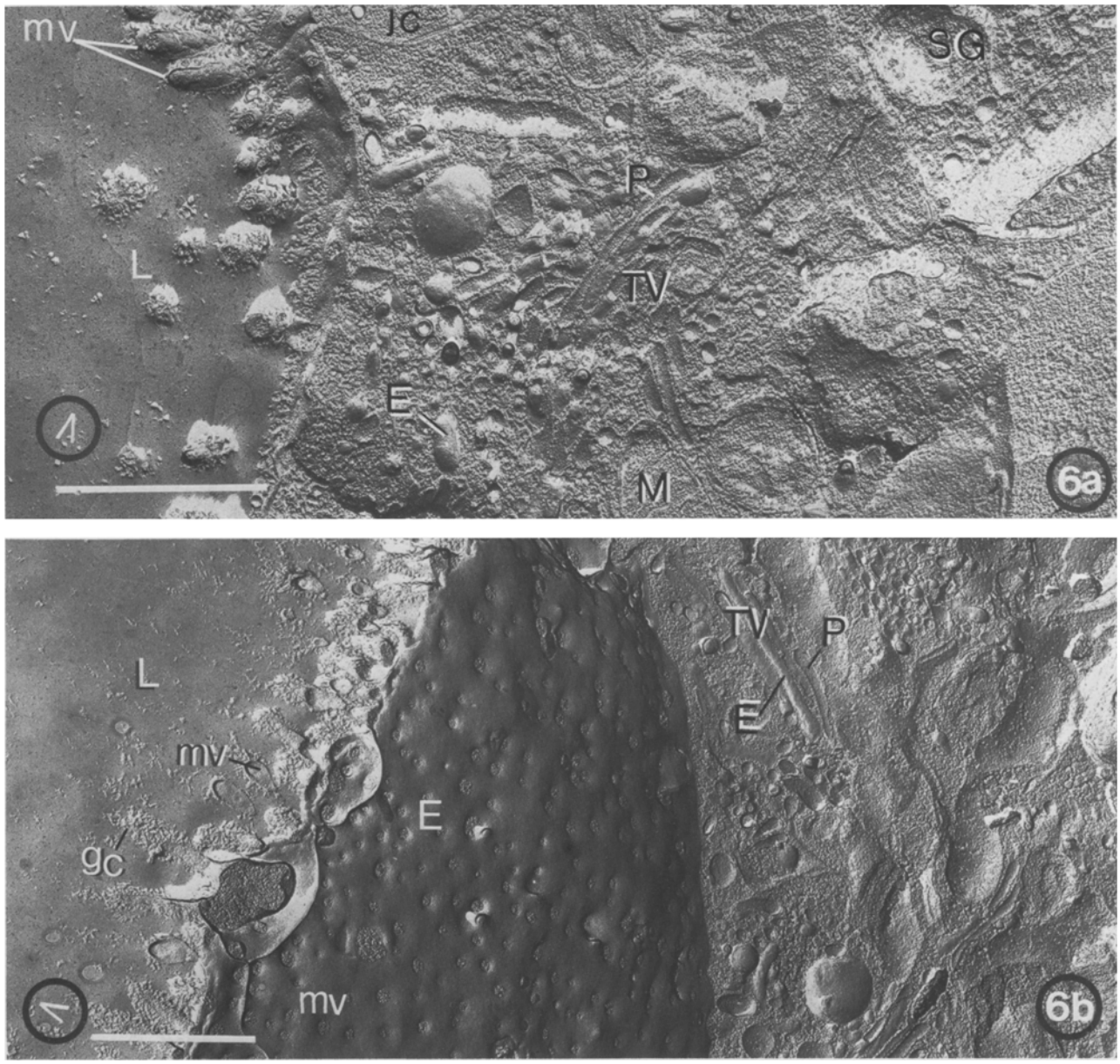

Fig. 6. Freeze-fracture replica of a toad oxyntic cell in the resting state. Detail of apical pole. (*a*) P faces of apical membrane and tubulovesicular system are observable. Fracture images of other organelles are seen. (*b*) Large area of apical membrane is fractured, showing the E face. Cytoplasmic cores of microvilli are seen. Note image of fractured glycocalix (*gc*) on the surface of microvilli. *mv*, microvilli; *L*, lumen; *E*, E face; *P*, P face; *TV*, tubulovesicular system; *jc*, junctional complex. Arrow in lower left corner depicts angle of shadowing. Bar: 1 μm. Magnification: 32,500× (*a*), 25,000× (*b*)

6–8). In the resting state (Fig. 6), both fracture faces, P and E [3], of the various membranes can be observed. On the P face, the particle density varies depending on the membrane. It is very high in the membranes of the TV system but low in the apical plasmalemma and secretory granules. On the E faces, particle density is always low and no apparent differences could be observed between the various membranes, in particular between TV system and apical membrane. On the apical plasmalemma and its microvilli, a fibrillar structure was seen adhering to the external side. This might represent the fracture image of the glycocalix observed by transmission electron microscopy [13]. In the resting state, where large sheets of membranes could be fractured, no communication could be evidenced between the apical membrane and the TV system.

In the presecretory state the apical plasma

membrane appeared now largely increased in area by the presence of long and numerous finger-like processes (Fig. 7). In addition to the increase in area of the apical membrane, two striking differences could be observed as compared to the resting state. The first is a change in particle density of the P face of the apical membrane. It is now rich in intramembrane particles (IMP) with an apparent density like that of the P face of the TV system. The other interesting feature is the appearance on the P face of bulges devoid of particles in the microvilli of the apical membrane. An attempt to quantitate the frequency of this phenomenon is presented in Table 2. In about 60% of all microvilli showing the P face, IMP-free bulges could be observed. In some cases up to three bulges could be counted on a single microvillus. This is a minimal estimate of the frequency since only a fraction of the P face of each microvillus is observed. In the insert of Fig. 7, in addition to the particle-free bulges already described, a depression devoid of particles can also be observed. This type of image was also rather frequent in this state. No apparent changes in other structures could be observed with this technique.

Table 2. Quantification of IMP-free bulges in microvilli of oxyntic cells in the presecretory state

Number of mucosae	3
Cells examined	22
Microvilli counted[a]	158
Microvilli with bulges	94
Number of bulges observed	126

[a] Only microvilli exposing the P fracture face were taken into consideration.

The increase in apical membrane area reached a maximum in the secretory state (Fig. 8). The P face of microvilli and apical plasmalemma was rich in

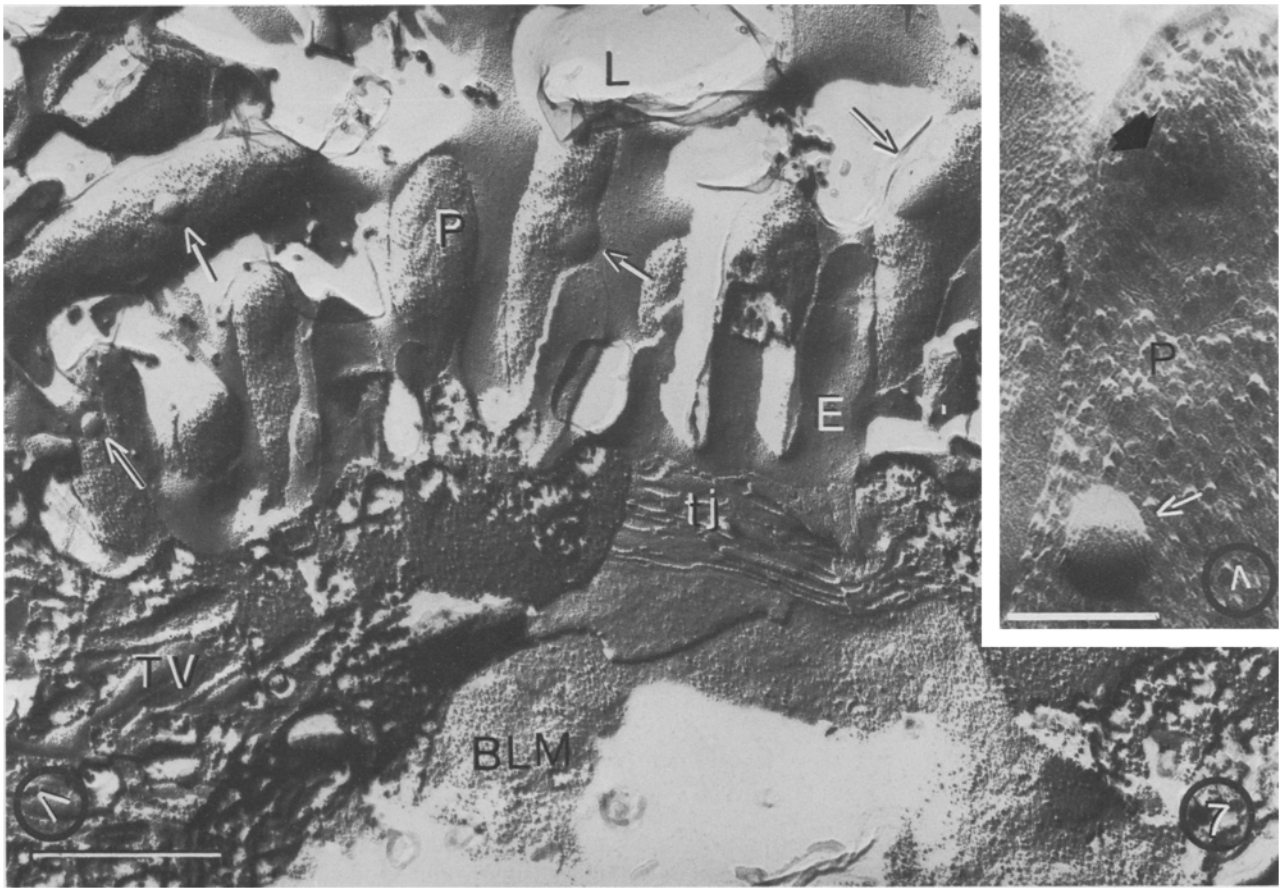

Fig. 7. Freeze-fracture replica of a toad oxyntic cell in the presecretory state. Detail of apical pole. Note numerous microvilli. IMP density of P face of apical membrane is similar to that of TV system. Arrows indicate IMP-free bulges on apical membrane. In the insert a detail of the P face of a microvillus is shown. Thin arrow indicates an IMP-free bulge. Thick arrow indicates a depression area devoid of IMP. *L*, lumen; *P*, P face; *E*, E face; *tj*, tight junction; *TV*, tubulovesicular system; *BLM*, basolateral membrane. Arrow at lower left corner depicts angle of shadowing. Bars: 1 μm and 0.1 μm (insert). Magnifications: 50,000× and 210,000× (insert)

particles with a density similar to that of the P face of the TV system. In this sense, the secreting oxyntic cell was like the one in the presecretory state. However, the particle-free bulges and depressions were never observed in this state. No apparent changes in other structures could be visualized in replicas of secreting oxyntic cells.

Studies with Horseradish Peroxidase

HRP was used in an attempt to visualize the sites of incorporation of extracellular space tracers. When the tissue was loaded with HRP, the electron-dense tracer penetrated into the pits and gland lumen. However, most of the HRP was localized in the pits associated with fibrillar material, probably mucus. In tissues that were loaded with HRP with the stimulation-inhibition sequence and left in the resting state only the oxyntic cells showed HRP localized intracellularly. In the resting oxyntic cell (Fig. 9) smooth membrane with microvilli typical of this state can be observed in unstained sections. No electron-dense material could be evidenced in the gland lumen. However, HRP was seen adhering to the surface of the apical membrane. Numerous tubular and vesicular profiles of elements of the TV system are seen. HRP is observed within many of

Fig. 8. Freeze-fracture replica of a toad oxyntic cell in the secreting state. Note increase in apical membrane area. *P*, P faces; *E*, E faces; *L*, lumen; *TV*, tubulovesicular system. Circled arrowhead depicts angle of shadowing. Bar: 0.5 μm. Magnification: 42,500×

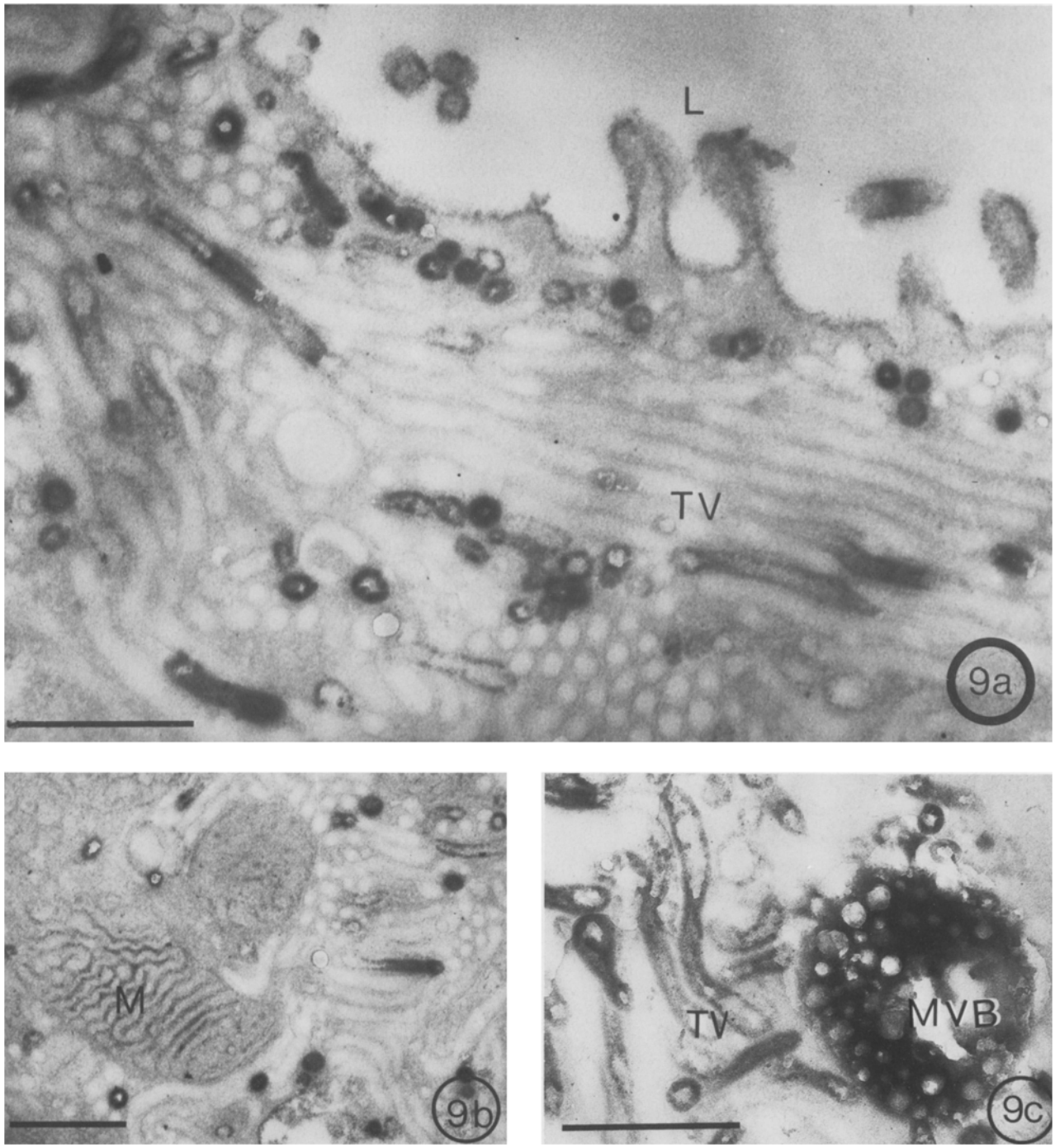

Fig. 9. Unstained section of a toad oxyntic cell in the resting state loaded with HRP. Numerous vesicular and tubular profiles are seen filled with electron-dense material. Endogenous reaction product is seen in mitochondrial christae (Fig. 9*b*). HRP is also seen in multivesicular bodies (Fig. 9*c*). *L*, lumen; *TV*, tubulovesicular system; *M*, mitochondria; *MVB*, multivesicular body. Bars: 0.5 μm. Magnifications: 59,400× (9*a*), 55,700× (9*b*) and 56,700× (9*c*)

these profiles. HRP was also observed within multivesicular bodies (Fig. 9*c*). Mitochondria showed a positive reaction in their cristae most probably due to endogenous peroxidase activity since it also appeared in tissues not loaded with exogenous HRP but treated with diaminobenzidine (Fig. 9*b*).

When HRP-loaded tissues were fixed shortly (5

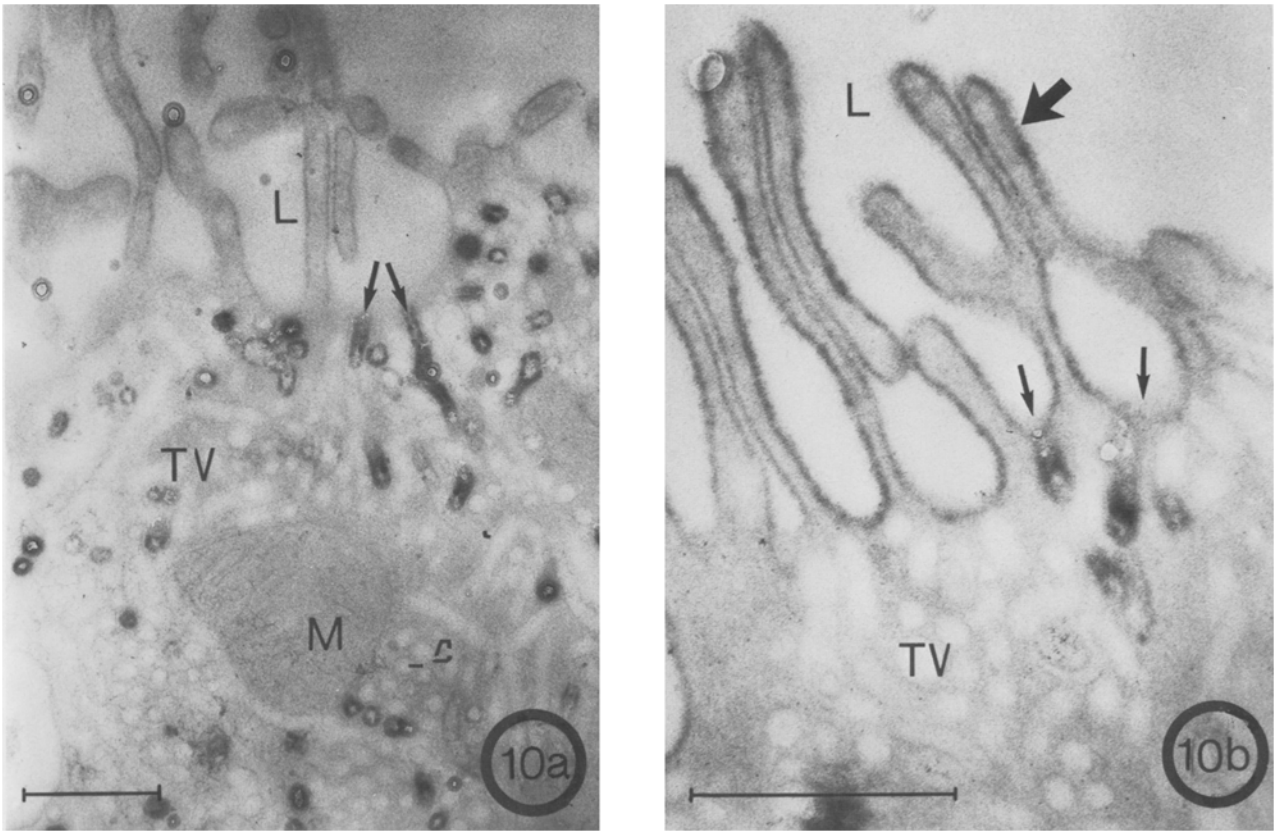

Fig. 10. Unstained sections of a toad oxyntic cell in the presecretory state. Mucosae had been loaded with HRP and then restimulated with db-cAMP (*see* Materials and Methods). Tubular profiles are seen in contact with the apical membrane or emptying into the lumen (thin arrows). HRP is seen adhering in some areas to the apical plasma membrane (thick arrow). *L*, lumen; *M*, mitochondria; *TV*, tubulovesicular system. Bars: 0.5 μm. Magnifications: 35,700× (*10a*), 69,300× (*10b*)

min) after restimulation, typical morphological changes were observed (Fig. 10). Long villi and foldings are seen in the gland lumen. At this stage, tubules are seen in contact with the apical membrane and some of them appeared to be emptying their contents into the lumen. HRP was also seen adhering to the exterior of the plasmalemma. Cells that had been stimulated for a longer time (45 min) showed typical changes induced by stimulation (Fig. 11). The amount of HRP seen in this case was much less than that observed in the resting state. However, HRP still remained in multivesicular bodies.

In another group of experiments, mucosae were brought to the resting state with metiamide. Then, they were exposed to HRP on the lumen side in the continuous presence of metiamide. These experiments served as a control for the nature of the incorporation of the tracer. HRP was observed adhering to the surface of the apical membrane, without filling the gland lumen as was the case for the preceding conditions. However, in this case, no electron-dense material was seen within the TV system or within multivesicular bodies.

Discussion

Stimulation of acid secretion in the gastric oxyntic cell of the vertebrate induces a proliferation of apical plasma membrane apparently at the expense of the intracellular TV system [16]. This process is reversible when the cell goes back to the resting state in each secretory cycle. Forte et al. [14] have proposed that retrieved membranes may be reutilized. Our results presented here are fully consistent with a membrane recycling hypothesis. In the present paper, we found that radioactive and electron-dense extracellular markers were incorporated into the TV system during membrane retrieval. Upon a new stimulation of secretion, markers were discharged to the luminal side. This was accompanied by an increase in membrane area. The morphological transformation after stimulation preceded

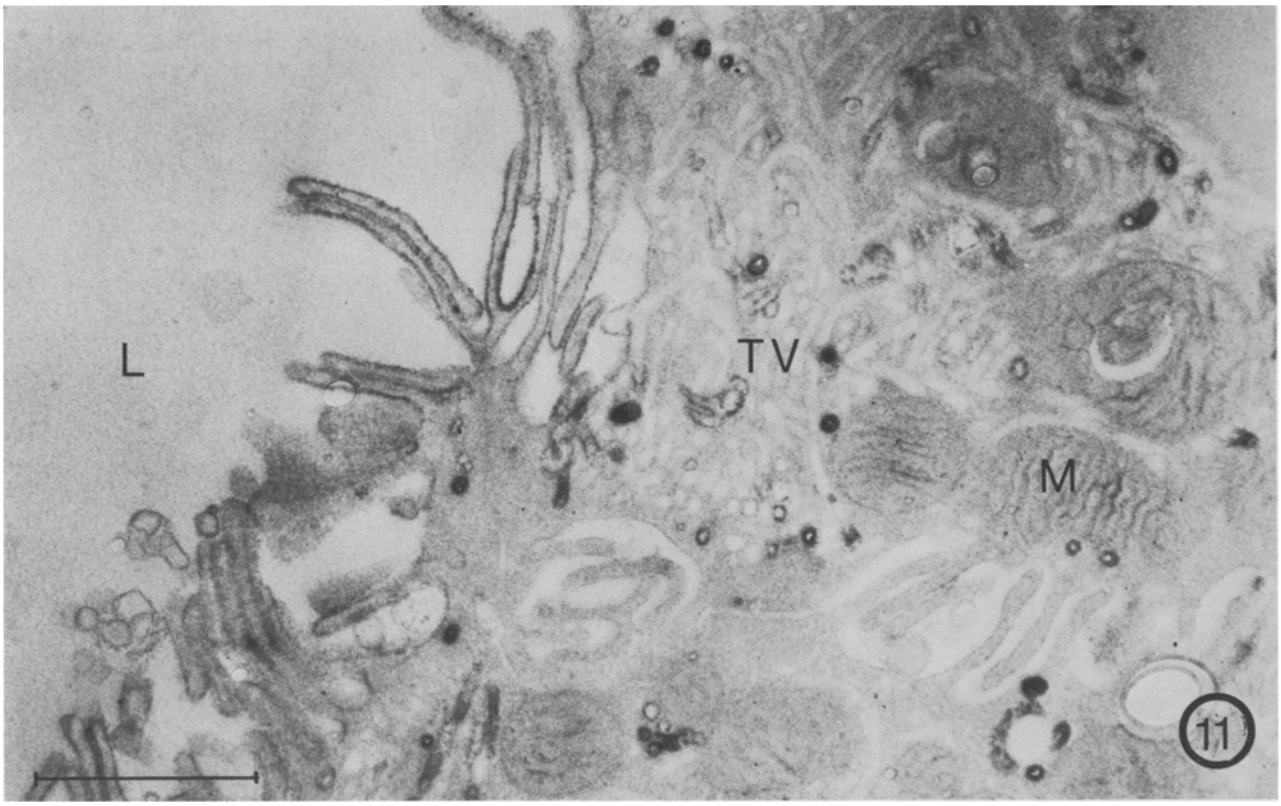

Fig. 11. Unstained section of a toad oxyntic cell in the secreting state. Mucosa had been preloaded with HRP and then restimulated with dc-cAMP and fixed 45 min after. *L*, lumen; *TV*, tubulovesicular system; *M*, mitochondria. Bar: 1 μm. Magnification: 29,050×

the onset of acid secretion as could be evidenced by efflux of radioactive markers and transmission and freeze-fracture electron microscopy. A membrane fusion mechanism appears to be involved in the increase in membrane area.

To interpret the results obtained with ^{14}C-inulin it was important to estimate the amount of tracer that reaches the bottom of the gland. Given its anatomy we need to consider the "sweeping out" effect produced by the net flow of water accompanying acid secretion [25, 28]. In this case, the water flow going out of the gland would oppose the diffusional entry of the tracer. Therefore, the relation of concentrations in the bulk solution and at any given length along the gland lumen in the steady state would be given by the following expression [25, 28]:

$$C/Co = e^{-vx/D}$$

where C is the concentration of the tracer at any length x along the gland; Co is the concentration of the tracer in the bulk solution, v is the velocity of secretory flow and D is the diffusion coefficient of the tracer in free solution. Assigning known values to these parameters (length of the gland, 200 μm [18]; velocity of secretion, 12 μl/cm^2 of gland lumen per hour [39] and D_{inulin}, 1.7×10^{-6} cm$^2 \cdot$ seg^{-1} [22]), we get an estimate of C/Co at the bottom of the gland of 0.68. This would be a minimum value for the bottom of the gland. We have manipulated the only parameter susceptible to modification which is the velocity of water flow. It has been shown [6] that the net water flow that accompanies acid secretion can be abolished or even reversed by placing an osmotic gradient across the tissue. In the present study we have used an osmotic gradient during the loading period to optimize availability of tracer along the gland. Furthermore, the return to the resting morphology after metiamide inhibition appears to be slower than cessation of H^+ secretion [40]. Thus, uptake of tracer would occur in a situation of zero or very little volume flow.

In the present study we were able to show uptake of electron-dense markers into the TV system during the reversal of the process and we could infer from this that also the radioactive markers were incorporated into the TV system. Uptake of fluid phase markers such as radioactive [27] and elec-

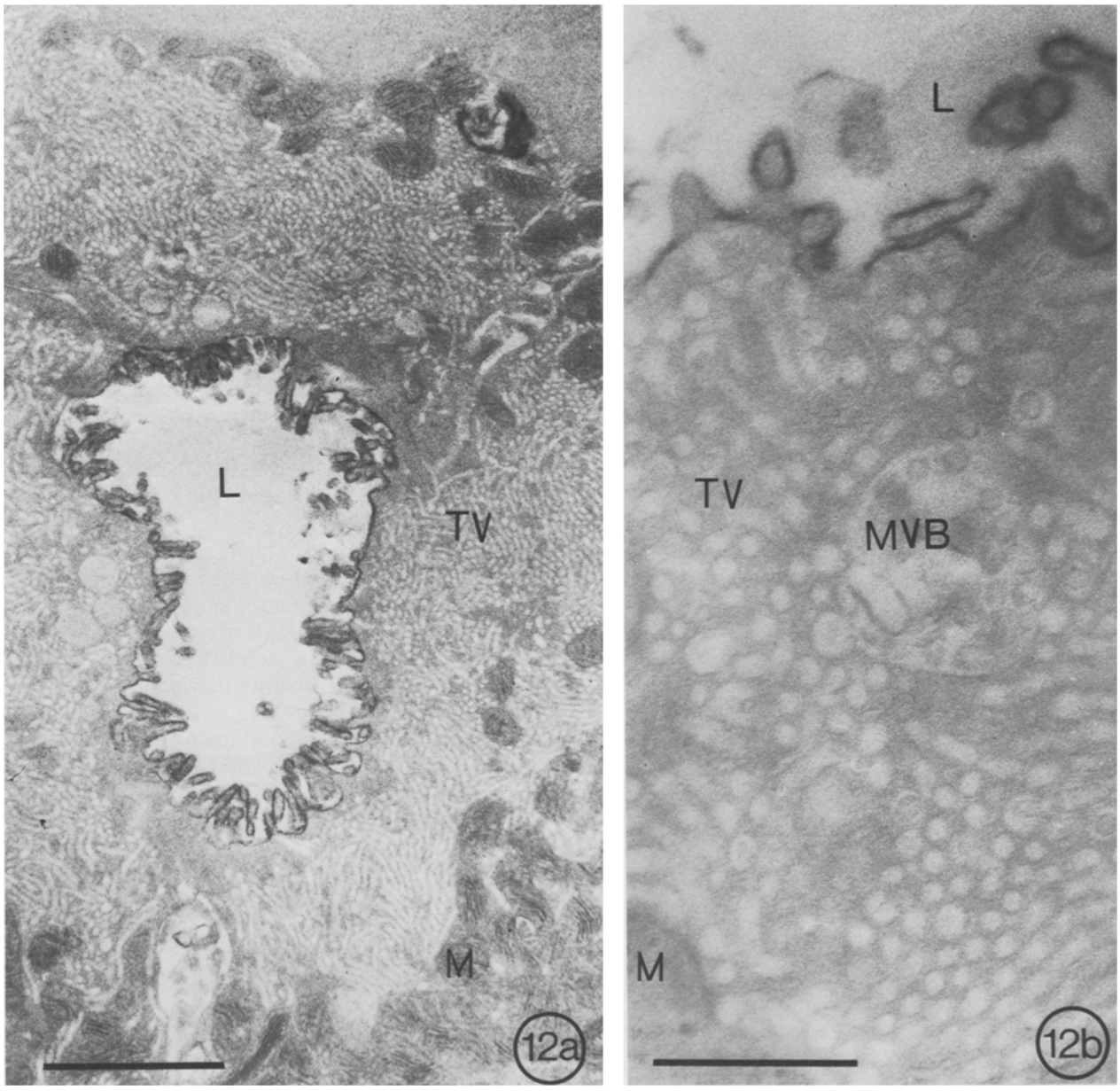

Fig. 12. Unstained sections of a toad gastric gland at the oxyntic cell region in the resting state. Resting mucosa was incubated with HRP in the luminal side for 90 min and then fixed. Electron-dense material is only seen adhering to the surface of the apical membrane. Endogenous reaction product is seen in mitochondrial christae. HRP is absent in the TV system or in multivesicular bodies. *L*, lumen; *TV*, tubulovesicular system; *M*, mitochondria; *MVB*, multivesicular body. Bars: 2 μm (12*a*); 0.5 μm (12*b*). Magnification: 13,500× (12*a*), 59,400× (12*b*)

tron-dense markers [21] during membrane retrieval has already been shown in a variety of systems [38]. In this tissue, Sedar [34] showed that HRP could be incorporated into the TV system of the oxyntic cell. On the other hand, Forte and Forte [12] showed in fixed tissues that lanthanum did not penetrate into the TV system in the resting oxyntic cell, and very poorly in the stimulated one. These results agree with our interpretation as will be discussed below, that there is no static communication between the TV system and the gland lumen. The fact of finding HRP in the TV system of a resting cell after reversal of the secretory state suggests that these structures are regenerated after membrane retrieval. Forte et al. [10] have shown incorporation of microperoxidase into endocytic and multimembrane vacuoles

in the mammalian parietal cell. The steps for the regeneration of the TV system after retrieval in the amphibian oxyntic cell are not known. However, it may involve the formation of intermediate structures similar to those seen in the parietal cell [10, 14, 16]. In other secretory cells (exocrine, endocrine and immunoglobulin-secreting cells), retrieved membranes fuse with Golgi cisternae to be reused as membrane containers in secretory granules for export of products (for a review *see* reference 9). On the other hand, the presence of HRP in multivesicular bodies and lysosomes may indicate that a certain degree of catabolism of membranes occurs after retrieval, at least in the presence of HRP. In control mucosae that were loaded with the tracer in the metiamide-inhibited state, no efflux of counts was observed. Also, no HRP was observed in the TV system when the mucosae were exposed to the electron-dense marker in inhibited condition. In this case HRP reached only the lumen of the gland. These results indicate that the loading of the TV system occurs only during retrieval of membranes.

The results obtained following restimulation were characterized by an increase in ^{14}C-inulin efflux whose onset and maximum preceded the onset and maximum of acid secretion. Furthermore, much of the increase in apical membrane area had already taken place at a time after stimulation corresponding with the peak of ^{14}C-inulin efflux and with no H^+ secretion. Similar observations have been made by electron microscopy in the mammalian stomach [17]. This result would indicate that the onset of the morphological transformation precedes the activation of the H^+ pump and might be a requirement for secretion. Our results with inulin efflux and morphology also suggest that the TV system does not contain a low pH fluid. Otherwise, H^+ would have accompanied or even preceded ^{14}C-inulin efflux. One can calculate the amount of acid that would be released if the volume of the TV system were full of isotonic HCl and then emptied into the lumen upon the morphological transformation. Based on our data (Table 1) we find that about 0.36 μeq would be released with ^{14}C-inulin at the time of the morphological transformation. If this transformation occurred in 20 min, the increase in H^+ secretion would be of about 1 μeq/hr. This change in secretory rate would accompany or even precede inulin efflux (H^+ diffuses faster than inulin) and would be easily detectable by our methods. Even if the whole process took one hour, the change in rate (of 0.36 μeq/hr) would still be detectable. In no case do we see an increase in H^+ rate of this magnitude accompanying ^{14}C-inulin efflux. Furthermore, the use of acridine orange fluorescence as an indicator of pH in mucosal slices of several amphibian species shows the accumulation of acid in the gland lumen upon stimulation. Regions of high acidity are absent in oxyntic cells in the resting state [37]. This, again, argues against the existence of preformed acid. Our results are in contrast with the findings in isolated gastric glands. Accumulation of aminopyrine and acridine orange fluorescence is consistent with regions of high H^+ activity within the cell, possibly the TV system in the resting state [1]. This might be a characteristic of the isolated gastric gland of the rabbit. The results in the *in vivo* dog stomach are consistent with the model here proposed for the amphibian [17].

The observations of marker efflux and images of HRP discharge into the lumen, accompanying the morphological transformation with restimulation of secretion, strongly suggest that at least an important fraction of the retrieved membranes are reutilized in the next secretory cycle.

The mechanism by which the area of the apical plasmalemma increases at the expense of the TV system is not known. A mechanism implying eversion of the TV system was early proposed by Sedar [33]. Recent results in isolated gastric glands [1] have been interpreted within the framework of this eversion hypothesis. In this case, the TV system membranes would be continuous with the apical plasmalemma and there would be communication between their lumen and the gland lumen. Stimulation would lead to a "turning-out" of this membranous element resulting in the morphological change. On the other hand, a second mechanism involving fusion of the TV system with the apical plasmalemma, as a consequence of stimulation, has been proposed [10, 11]. The results shown in this paper rather support the fusion hypothesis. Images suggestive of fusion observed by transmission electron microscopy appeared in the presecretory state. These images in the toad are similar to those observed by many authors in other species. When the tissue was observed in the same state by freeze-fracture electron microscopy we found images that have been associated with membrane fusion in other systems. Thus, bulges devoid of IMP on the P fracture face were observed on the newly formed finger-like processes and membrane proliferations. Similar structures have been described in other secretory systems at the time and place of membrane fusion [24]. More recently, Chandler and Heuser [5], from their studies in quick-frozen cells, have argued that these IMP-free bulges may be artifacts only seen in fixed tissues, although they most probably originate at early stages of membrane fusion. The fact that these images appear only in the presecretory state, at the places of membrane contacts

seen in transmission electron microscopy, and coinciding with radioactive tracer efflux, makes it highly likely that they represent points of membrane fusion. Furthermore, the complete absence of communication between the TV system and the apical plasma membrane in the resting state argues against the possibility of an eversion of the TV system.

The results obtained in this paper, with different approaches and techniques, are consistent with a model where the increase in apical membrane area, following stimulation, occurs by a fusion mechanism. This transformation would precede the onset of secretion and would be a requirement for it. Upon withdrawal of the stimulus or inhibition, the apical membrane would be retrieved by endocytosis with the consequent regeneration of the TV system. Retrieved membranes could be then recycled.

We are deeply indebted to Marie-Christine Ruiz for her unrestricted collaboration throughout all the stages of this work. We also thank Dr. Francisco Gil for his collaboration in the freeze-fracture studies. The expert secretarial assistance of Miss Isabel Otaegui is gratefully acknowledged.

References

1. Berglindh, T., DiBona, D.R., Ito, S., Sachs, G. 1980. Probes of parietal cell function. *Am. J. Physiol.* **238:**G165–G176
2. Black, J.W., Duncan, W.A.M., Durant, G.J., Ganellin, C.R., Parsons, M.E. 1972. Definition and antagonism of histamine H_2 receptors. *Nature (London)* **236:**385–390
3. Branton, D., Bullivant, S., Gilula, N.B., Karnovsky, M.J., Moor, H., Muhlethaler, K., Northcote, D.H., Packer, L., Satir, B., Satir, P., Speth, V., Staehlin, L.A., Steere, R.L., Weinstein, S.R. 1975. Freeze-etching nomenclature. *Science* **190:**54–56
4. Carlisle, K.S., Chew, C.S., Hersey, S.J. 1978. Ultrastructural changes and cyclic AMP in frog oxyntic cells. *J. Cell Biol.* **76:**31–42
5. Chandler, D.E., Heuser, J.E. 1980. Arrest of membrane fusion events in mast cells by quick-freezing. *J. Cell Biol.* **68:**666–674
6. Durbin, R.P., Frank, H., Solomon, A.K. 1965. Water flow through frog gastric mucosa. *J. Gen. Physiol.* **39:**535–551
7. Durbin, R.P., Heinz, E. 1958. Electrogenic chloride transport and gastric acid secretion in the frog. *J. Gen. Physiol.* **41:**1035–1047
8. Farquhar, M.G. 1978. Recovery of surface membrane in anterior pituitary cells. *J. Cell Biol.* **77:**R35–R42
9. Farquhar, M.G. 1981. Membrane recycling in secretory cells: Implications for traffic of products and specialized membranes within the Golgi complex. *In:* Methods in Cell Biology. A.R. Hand and C. Oliver, editors. Vol. 23, pp. 399–427. Academic, New York
10. Forte, J.G., Black, J.A., Forte, T.M., Machen, T.E., Wolosin, J.M. 1981. Ultrastructural changes related to functional activity in gastric oxyntic cells. *Am. J. Physiol.* **241:**G349–G358
11. Forte, J.G., Forte, T.M., Ray, T.K. 1972. Membranes of the oxyntic cell: Their structure, composition and genesis. *In:* Gastric Secretion. G. Sachs, E. Heinz and K.J. Ulrich, editors. pp. 37–67. Academic, New York
12. Forte, T.M., Forte, J.G. 1970. Definition of the extracellular space in secreting and nonsecreting oxyntic cells. *J. Cell Biol.* **74:**782–786
13. Forte, T.M., Forte, J.G. 1970. Histochemical staining and characterization of glycoproteins in acid-secreting cells of frog stomach. *J. Cell Biol.* **47:**437–452
14. Forte, T.M., Machen, T.E., Forte, J.G. 1977. Ultrastructural changes in oxyntic cells associated with secretory function: A membrane-recycling hypothesis. *Gastroenterology* **73:**941–955
15. Frexinos, J., Carballido, M., Louis, A., Ribet, A. 1971. Effects of pentagastrin stimulation on human parietal cell. An electron microscopy study with quantitative evaluation of cytoplasmic structures. *Am. J. Dig. Dis.* **16:**1065–1074
16. Helander, H.F., Hirschowitz, B. 1972. Quantitative ultrastructural studies on gastric parietal cells. *Gastroenterology* **63:**951–961
17. Helander, H.F., Hirschowitz, B. 1974. Quantitative ultrastructural studies on inhibited and on partly stimulated gastric parietal cells. *Gastroenterology* **67:**447–452
18. Helander, H.F., Sanders, S.S., Rehm, W.S., Hirschowitz, B.I. 1972. Quantitative aspects of gastric morphology. *In:* Gastric Secretion. G. Sachs, E. Heinz and K.J. Ullrich, editors. pp. 69–88. Academic, New York
19. Herzog, V., Farquhar, M.G. 1977. Luminal membrane retrieved after exocytosis reaches most Golgi cisternae in secretory cells. *Proc. Natl. Acad. Sci. USA* **74:**5073–5077
20. Heuser, J.E., Reese, T.S., Dennis, M.J., Jan, Y., Jan, L., Evans, L. 1979. Synaptic vesicle exocytosis captured by quick freezing and correlated with quantal transmitter release. *J. Cell Biol.* **81:**275–300
21. Heuser, J.E., Reese, T.S. 1973. Evidence for recycling of synaptic vesicle membrane during transmitter release at the frog neuromuscular junction. *J. Cell Biol.* **57:**315–344
22. International Critical Tables. 1929. Vol. V., p. 63. McGraw-Hill, New York
23. Kasbekar, D.K. 1967. Studies of resting isolated frog gastric mucosa. *Proc. Soc. Exp. Biol. Med.* **125:**267–270
24. Lawson, D., Raff, M.C., Gomperts, B., Fewtrell, C., Gilula, N.B. 1977. Molecular events during membrane fusion. A study of exocytosis in rat peritoneal mast-cells. *J. Cell Biol.* **72:**242–259
25. Moody, F.G., Durbin, R.P. 1969. Water flow induced by osmotic and hydrostatic pressure in the stomach. *Am. J. Physiol.* **217:**255–261
26. Moor, H., Mühlethaler, K. 1963. Fine structure in frozen-etched yeast cells. *J. Cell Biol.* **17:**609–627
27. Nordmann, J.J., Dreifuss, J.J., Baker, P.F., Ravazzola, M., Malaisse-Lagae, F., Orci, L. 1974. Secretion-dependent uptake of extracellular fluid by the rat neurohypophysis. *Nature (London)* **50:**155–157
28. Rehm, W.S., Schlesinger, H., Dennis, W.H. 1953. Effect of osmotic gradients on water transport, hydrogen ion and chloride ion production in the resting and secreting stomach. *Am. J. Physiol.* **175:**473–486
29. Ripps, H., Shakis, M., MacDonald, E.D. 1976. Peroxidase uptake by photoreceptor terminals of the skate retina. *J. Cell Biol.* **70:**86–96
30. Sachs, G., Shoemaker, R., Hirschowitz, B.I. 1967. The action of amytal on frog gastric mucosa. *Biochim. Biophys. Acta* **143:**522–531

31. Schacher, S., Holtzman, E., Hood, D.C. 1976. Synaptic activity of frog retinal photoreceptors. A peroxidase uptake study. *J. Cell Biol.* **70:**178–192
32. Sedar, A.W. 1962. The fine structure of the oxyntic cell in relation to functional activity of the stomach. *Ann. N.Y. Acad. Sci.* **99:**9–29
33. Sedar, A.W. 1965. Fine structure of the stimulated oxyntic cell. *Fed. Proc.* **24:**1360–1367
34. Sedar, A.W. 1969. Uptake of peroxidase into the smooth-surfaced tubular system of the gastric acid secreting cell. *J. Cell Biol.* **43:**179–184
35. Sedar, A.W., Forte, J.G. 1963. The effect of thiocyanate on the fine structure of the oxyntic cell in bullfrog *in vitro* gastric mucosa. *Anat. Rec.* **145:**283–284
36. Shoemaker, R.L., Buckner, E., Spenney, J.G., Sachs, G. 1974. Action of Burimamide, a histamine antagonist, on acid secretion *in vitro*. *Am. J. Physiol.* **226:**898–902
37. Shoemaker, R.L., Ruiz, M.C., Michelangeli, F. 1983. Intracellular potentials of bullfrog fundic gastric mucosa, *in vitro*. *Fed. Proc.* (*Abstract*) (*In press*)
38. Steinman, R.M., Mellman, I.S., Muller, W.A., Cohn, Z.A. 1983. Endocytosis and the recycling of plasma membrane. *J. Cell Biol.* **96:**1–27
39. Villegas, L. 1965. Efflux of chloride through cell surfaces of frog gastric mucosa. *Am. J. Physiol.* **208:**380–384
40. Zalewsky, Ch. A., Moody, F.G. 1977. Stereological analysis of the parietal cell during acid secretion and inhibition. *Gastroenterology* **73:**66–74

Received 22 August 1983; revised 18 November 1983